

1 **Running title:** Automatic Detection of Vessel Signatures in Audio Record-
2 ings with Spectral Amplitude Variation Signature
3 **Number of words:** ~6105
4 **Number of tables:** 3
5 **Number of figures:** 14
6 **Number of references:** 18

7 **Automatic Detection of Vessel Signatures in**
8 **Audio Recordings with Spectral Amplitude**
9 **Variation Signature.**

10 **Clausius Duque Gonçalves Reis^{1,2,*},**
11 **Linilson Rodrigues Padovese³,**
12 **Maria Cristina Ferreira de Oliveira².**

13 1. *Federal University of Viçosa (UFV-CRP) - Rio Paranaíba, MG.*
14 2. *University of São Paulo (ICMC-USP) - São Carlos, SP.*
15 3. *University of São Paulo (POLI-USP) - São Paulo, SP.*

16 *Correspondence author. clausius@ufv.br

Summary

1. Sound emissions by ships and boats can strongly impact marine life, with potential to affect communications, breeding and prey and predator relationships. Automatic detection of boat signatures in underwater audio recordings is thus an important task. Automated solutions are particularly relevant for monitoring preservation areas where the presence of watercrafts is usually regulated. The task is particularly challenging because it requires distinguishing multiple overlapping acoustic events in typically noisy audio recordings.
2. In this paper we introduce an algorithm for boat and ship detection which computes an acoustic signature that captures the variance in the frequency amplitudes observed over the duration of the signal.
3. We evaluated the algorithm on a database of underwater recordings collected at two conservation areas in the State of São Paulo, Brazil, with very good results, and also compared it with an existing solution.
4. Besides being effective, the algorithm requires limited user input and no parameter fine tuning to handle diverse situations. It thus provides a solution to automate the detection of vessels, with potential applications for monitoring marine preservation areas.

41 Keywords: Acoustic Ecology, Boat, DEMON, Detection, Signature, Sound-

42 scape, Spectrogram, Underwater

43 **Introduction**

44 Audio signals emitted by boats, ships and water crafts in general can strongly
45 impact marine life. They may interfere with species communication (Witte-
46 kind and Schuster, 2016), echolocation mechanisms (Veirs et al., 2016) and
47 threaten fish population growth (Jain-Schlaepfer et al., 2018).

48 Ecological audio recorders and hydrophones offer a cost effective method
49 for ocean monitoring in order to identify undesirable or threatening scenarios.
50 However, manual inspection of collections of audio recordings obtained over
51 extensive time periods is not feasible, in view of the time and human effort it
52 demands. This has motivated many research efforts towards devising meth-
53 ods to automatically detect the presence of vessels in underwater acoustic
54 recordings.

55 While some solutions have employed classification approaches derived
56 from the analysis of acoustic features (Leal et al., 2015), others have focused
57 on the specific spectral signatures of the sounds emitted by the different
58 types of vessels, e.g. training neural networks to detect a set of known signa-
59 tures (Pollara et al., 2017; Slamnoiu et al., 2016; Chung et al., 2011; Hanson
60 et al., 2008). Nonetheless, improving detection accuracy in noisy conditions
61 and reducing the rate of false positives remain as challenges. A related rel-
62 evant issue is automatic classification, e.g., categorizing the vessels detected,
63 for example, according to their size (small, medium, large).

64 The *Detection of Envelope Modulation On Noise* (DEMON) is one of
65 the most reliable methods for ship detection and classification (Chung et al.,
66 2011). However, it is reported to yield poor results on noisy signals. Moreover,

67 it is highly dependable on a manual selection of the relevant frequency band
68 pass filters for analysis, which must be tuned according to the type of target
69 vessel (Hanson et al., 2008).

70 In this work we introduce a novel method to automatically detect the
71 presence of boats or ships in acoustic underwater recordings. Similarly to the
72 DEMON method, ours relies on computing acoustic signatures from the input
73 signal. However, our method has lower computational cost and requires no
74 calibration or human intervention. Moreover, we show that it can successfully
75 detect vessels even in challenging conditions posed by very noisy signals, as
76 in recordings that include crustacean acoustic activity.

77 In the remainder of this paper, first we we discuss related research on
78 automatic vessel detection and characterization. Then we describe the tech-
79 nique developed, explaining its underlying rationale and presenting the al-
80 gorithm for signature computation and vessel detection. We present results
81 from employing the proposed algorithm to detect ships and small boats in
82 a database of underwater recordings collected at two protected sites on the
83 Brazilian coast. We also present results comparing the performance of our
84 method with an implementation of a DEMON-type signature, in terms of
85 quality and computational cost. Finally, we present conclusions and discuss
86 future work.

87 Related Work

88 A significant increase in the number of large vessels navigating the oceans
89 has motivated investigations on the effects of noise levels on marine life (Wit-

90 tekind and Schuster, 2016; Merchant et al., 2014).

91 Large vessels emit acoustic signals in the low frequency spectrum, the
92 same frequency bands used for communication by certain groups of animals,
93 such as baleen whales (Wittekind and Schuster, 2016). Noise due to ships
94 has also been found to disrupt the echolocation mechanism of endangered
95 species such as killer whales (Veirs et al., 2016).

96 A recent study suggested motorboats cause a stress response in fish em-
97 bryos (Jain-Schlaepfer et al., 2018), with an increase in their heart rate and
98 even stronger effects, depending on the engine type, e.g., two or four strokes.

99 The potential impact of underwater noise on marine mammals is widely
100 recognized. Merchant et al. (2014) characterized the natural and anthropo-
101 genic contributors to underwater noise, specifically in a conservation area
102 with increased shipping activity associated with offshore energy develop-
103 ments. They monitored ship activity using *Automatic Identification System*
104 (AIS), in which transponders send information about each ship present in
105 the area, in addition to video surveillance and automated sound recorders to
106 monitor noise levels. They correlated the data collected from those sources
107 to investigate the relationship between broadband sound exposure and in-
108 dicators proposed by the EU *Marine Strategy Framework Directive* to access
109 the effects of noise exposure over a locally protected bottlenose dolphin pop-
110 ulation. The authors determined that the bottlenose dolphin population is
111 not under current danger due to the current noise levels they are exposed,
112 however their study will serve as a baseline for future investigations on the
113 effect of noise levels on the local marine life.

114 The combination of low-cost automated acoustic recorders and algorithms

115 capable of detecting boats in long duration recordings can provide an effect-
116 ive solution to monitoring conservation areas for the presence of vessels. Leal
117 et al. (2015), for instance, introduced a method for boat classification based
118 on Fourier transform and signal processing to identify the occurrence of ves-
119 sels in the recordings.

120 Features extracted from the audio spectrum and fed to *Artificial Neural*
121 *Networks* (ANNs) and *Support Vector Machines* (SVMs) have been success-
122 fully employed to classify ships according to their type (Leal et al., 2015). A
123 10-dimensional feature array was created, given by the highest peak value in
124 the original audio signal plus eight values corresponding to the energies of
125 the first eight 500-Hz segments, and the central frequency of the smoothed
126 signal. Leal et al. (2015) argue that acoustic emissions by vessels are too
127 complex to be analyzed directly from the raw form of the signal’s discrete
128 Fourier transform.

129 Averbuch et al. (2011) rely on wavelet packet coefficients to detect cer-
130 tain types of vessel in recordings with background noise. They derive acoustic
131 signatures using a combination of a Linear Discriminant Analysis (LDA) clas-
132 sifier with Classification and Regression Trees (CART), plus an additional
133 component to reduce false alarms. Automatic real-time detection requires a
134 training step with a set of pre-registered signatures of interest, where the sig-
135 natures are generated from “energy maps” derived from the blocks of “wavelet
136 packet coefficients”.

137 The method by Yan et al. (2017) uses a combination of resonance-based
138 sparse signal decomposition (RSSD) and Hilbert marginal spectrum (HMS)
139 analysis to recognize certain types of vessels, defined *a priori*. The authors

140 use an RSSD decomposition of the original audio signal to separate it into
141 high and low resonance signals, corresponding respectively to the target and
142 background noise. Hilbert-Huang transform (HHT) is applied to extract
143 characteristics from the purified audio and SVM is employed for signal clas-
144 sification. Gaussian white noise was added to the recordings in different
145 proportions to perform the decomposition tests and obtain the boat signa-
146 tures.

147 Both previous solutions demand transformations of the original signal,
148 e.g., employing RSSD or waveletets, and are targeted at the problem of
149 categorizing the vessel signatures against a predefined set of classes. The
150 solution proposed in this paper to compute vessel signatures does not re-
151 quire complex transformations of the original signal, as it relies directly on
152 its FFT frequency spectrum. Moreover, it is aimed at detecting the pres-
153 ence of acoustic events introduced by arbitrary types of vessels in the audio
154 recordings, without performing classification.

155 A well-known method for vessel detection in audio recordings is the *De-*
156 *tection of Envelope Modulation On Noise* (DEMON) algorithm. By enhan-
157 cing audio frequencies characteristic of vessel emissions it creates an acous-
158 tic signature that can be employed for classification (Pollara et al., 2017,
159 2016; Chung et al., 2011). Introduced over 50 years ago (Tuteur, 1963), the
160 DEMON signature has inspired several novel ship classification algorithms
161 (Chung et al., 2011).

162 A recent study compared four DEMON-type algorithms (Slamnoiu et al.,
163 2016) regarding their ability to detect small ships and divers, as well as their
164 robustness to acoustic noise. The same authors (Slamnoiu et al., 2016) in-

165 introduced a variation of the classic algorithms that was shown to yield similar
166 results with less computational effort, also arguing that their modified DE-
167 MON algorithm is more robust to noise.

168 Chung et al. (2011) described an approach for identification and classifica-
169 tion of multiple ships in busy harbor conditions using the DEMON algorithm.
170 Employing a system consisting of four hydrophones, the authors used cross-
171 correlation to compute the delay between the corresponding recordings and
172 could even estimate the relative positions of the boats. Chung et al. (2011)
173 state that ship detection and classification are governed by the propeller and
174 by engine parameters such as number of blades and rotational speed. As
175 such, the audio spectrum is one of the most reliable acoustic parameters to
176 accomplish such tasks. A major limitation of approaches that rely on the
177 standard DEMON algorithm is that human intervention is required to ob-
178 tain good results. For instance, the user must select a suitable band pass
179 filter to recognize a specific signature.

180 In order to improve the resolution of the resulting DEMON algorithm
181 and increase the capability of detecting subtle details within the recordings,
182 Hanson et al. (2008) used cyclostationary signal processing, exploiting the
183 spectral redundancy inherent to the propeller signal. This enhancement en-
184 abled blind identification of the shaft speed and number of propeller blades,
185 even in noisy signal conditions. This modification improved signal resolution
186 and allowed identifying the presence of multiple vessels. Emission by snap-
187 ping shrimps is, according to the authors, a major source of noise that can
188 render methods based on the DEMON signature ineffective.

189 Several relevant contributions previously discussed relied on the DEMON

190 algorithm and variations therein. Nonetheless, besides its sensitivity to cer-
191 tain types of noise, computing a DEMON signature from raw audio signals
192 requires non-trivial levels of human intervention. The solution introduced in
193 this paper adopts a different strategy to obtain an acoustic signature, which is
194 simpler than the DEMON signature, practically eliminating the need of user
195 intervention during the extraction and detection processes. Our tests, per-
196 formed on audio recordings collected at marine ecological conservation areas
197 with intense crustacean acoustic activity, indicate that the technique can
198 successfully detect the presence of different types of boats and also identify
199 their corresponding acoustic signatures.

200 **Materials and Methods - Spectral Amplitude**

201 **Variation Signature for Vessel Detection**

202 A first step in automatic detection of boats, ships and other types of water
203 crafts in underwater acoustic recordings is to distinguish their acoustic signa-
204 tures from those due to natural elements such as fish choruses or crustacean
205 acoustic activity. Audio signals emitted by vessels can be characterized by
206 narrow stationary frequency signatures, as the engine, propellers and cavita-
207 tion produce sounds that usually remain stable along the duration of a single
208 recording.

209 The audio spectrograms shown in Figure 1 illustrate occurrences of three
210 acoustic events captured underwater, namely boats, indicated by the red
211 squares, fish choruses, indicated by the blue squares and background noise

212 from crustaceans, visually perceptible as vertical lines in both spectrograms.
213 The spectral signatures of both the fish choruses and the boats are charac-
214 terized by frequency peaks that persist along extensive time periods. Even
215 though they may appear similar, the frequency peaks due to boats appear
216 over narrow frequency bands, unlike the fish choruses, which are observed
217 over wider bands. The distinction poses a challenging scenario for automatic
218 boat detection, as boats and fish choruses can be easily mistaken, and boat
219 events may be totally masked by strong background noise.

220 Our proposed method for automatic vessel detection in underwater eco-
221 logical recordings considers certain unique features of the sounds emitted by
222 vessels to discern their characteristic frequency peaks from those produced
223 by other acoustic events. The algorithm considers as input the *dB* frequency
224 spectrum of the audio signal segmented into one-minute audio samples. It
225 initially computes a so-called **frequency amplitude variation** (FAV) sig-
226 nature from each one-minute segment of the audio spectrum.

227 The overall process, as well as the motivation for our choices in deriving
228 the proposed algorithm are detailed next. Unlike the DEMON method, which
229 considers the audio envelope of the signal, our algorithm relies on information
230 obtained from the audio spectrogram matrix. The audio spectrogram is
231 computed with the *Short-Time Fourier Transform* (STFT), using as input
232 the audio signal and an *FFT size*, which was established as 11025, equal to the
233 audio sampling rate, in order to yield a nominal frequency resolution of 1Hz
234 while resulting in one FFT sample per second. The resulting spectrogram
235 matrix thus has $F = (11025/2)$ frequencies and $S = (N \times 60)$ samples, or one
236 sample for each second of the input audio, where N is the audio duration, in

237 minutes. Our analyses have been conducted on 15-minute recordings.

Algorithm 1 describes the necessary steps to obtain the FAV signature and the corresponding boat detection signature.

Algorithm 1: FAV signature computation

Input:

```
1 Sample[0..60][0..Rate/2]    ▷ 1-Minute Spectrogram matrix
 2 Rate                      ▷ Audio sampling rate
 3 MaxFreq                  ▷ Maximum frequency of analysis
 4 SDMultiplier             ▷ SD threshold multiplier
```

Result:

4 FAV ▷ Frequency Amplitude Variation signature
5 BoatDetection ▷ Boat detection signature

```

6 Mean[0..Rate/2]  $\leftarrow$  frequencyMean(Sample)
7 SmoothMean[0..Rate/2]  $\leftarrow$  smooth(Mean, blackman, 8)
8 SD  $\leftarrow$  StandardDeviation(SmoothMean)

```

9 $Mean \leftarrow Mean[0..MaxFreq]$

10 $SmoothMean \leftarrow SmoothMean[0..MaxFreq]$

11 $FAV[0..MaxFreq] \leftarrow 0$

12 $BoatDetection[0..MaxFreq] \leftarrow 0$

13 **for** $i \leftarrow 0$ **to** $MaxFreq$ **do**

14 | variation \leftarrow SmoothMean[i] – SmoothMean[i – 1]

18 $FAV[i] \leftarrow |(variation)^3|$

19 | if $FAV[i] > (SD \times SDMultiplier)$ then

20 | *BoatDetection*[*i*] \leftarrow 1

end

end

23 *BoatDetection*[0..20] \leftarrow 0

24 *BoatDetection* $[(MaxFreq - 10)..MaxFreq] \leftarrow 0$

25 **return** *FAV, BoatDetection*

241 As described, the spectrogram matrix covers N one-minute samples of
242 the audio recording. The frequency amplitudes of each one-minute sample

243 are averaged in order to obtain a single representative frequency amplitude.
244 The result is a spectrum signature of the one-minute audio segment stored
245 in an array of size F , where each entry corresponds to an average frequency
246 amplitude (Algorithm 1, lines 6-7). Computing the average spectrum signa-
247 ture of one-minute audio samples, instead of the entire audio, avoids missing
248 short duration events. It also allows precisely locating the events along the
249 audio duration, which is useful for analysis and visualization purposes.

250 The spectrum signature is the input to the FAV signature computation,
251 which is at the core of the boat detection procedure. The size of the spectrum
252 signature is equal to the maximum frequency component in the recording, as
253 it has been obtained considering F , however it can be set to a maximum fre-
254 quency of analysis (Algorithm 1, lines 9-10). The spectrum signature is thus
255 stored in an array in which each entry corresponds to a frequency window
256 of 1Hz. Let $SmoothMean[0...F - 1]$ denote the array storing the smoothed
257 spectrum signature, with F values. It is possible to compute the differences
258 between each pair of frequency amplitudes in the signature, applying Equa-
259 tion 1 to each element in this array (Algorithm 1, lines 14-16).

$$FAV_f = |(SmoothMean_f - SmoothMean_{f+1})^3| \quad (1)$$

260 Equation 1 yields the unsigned differences between consecutive frequency
261 pairs of the input signal (Algorithm 1, line 18). The resulting differences,
262 raised to power 3, are stored as elements of a new array FAV , of size $F - 1$,
263 which stores the FAV signature. The reason for raising the resulting differ-
264 ences to power 3 is to emphasize the frequency peaks due to boats against the

265 peaks due to other events that also introduce frequency amplitude variations.
 266 Raising to other power values could yield a similar effect, but empirical in-
 267 vestigations led us to this choice.

268 The FAV signature captures and emphasizes persistent variations in the
 269 frequency amplitudes contained in the input spectrum. Such variations can
 270 yield a single peak or multiple frequency peaks, resulting in different patterns
 271 characteristic of certain acoustic events, including boats. Our goal is thus to
 272 identify the peak patterns characteristic of acoustic emissions by boats.

273 A threshold of $\alpha = 1.5 \times \text{Standard Deviation}$ of the original spectrum has
 274 been empirically found suitable to identify the frequency peak patterns due
 275 to boats, even in noisy conditions. The algorithm applies this threshold to
 276 the FAV signature (Algorithm 1, lines 19-20) to yield a binary boat detection
 277 signature array, also of size $F - 1$, applying Equation 2:

$$\text{BoatDetection}_f = h(\text{FAV}_f, \alpha) \quad (2)$$

278 where

$$h(\text{FAV}_f, \alpha) = \begin{cases} 1, & \text{if } \text{FAV}_f \geq \alpha \\ 0, & \text{otherwise} \end{cases} \quad (3)$$

$$\alpha = \left(\sqrt{\frac{1}{n} \sum_{i=1}^n (\text{SmoothMean}_i - \mu)^2} \right) \times 1.5 \quad (4)$$

$$\mu = \left| \frac{1}{n} \sum_{i=1}^n \text{SmoothMean}_i \right| \quad (5)$$

279 The result is a binary array *BoatDetection*, in which each entry is flagged
280 to 1 whenever the corresponding entry in the FAV signature array is above
281 the threshold ($SmoothMean_n > \alpha$), signalling this as a peak indicative of
282 the presence of a boat, otherwise the corresponding array entry remains set
283 as 0.

284 The acoustic events introduce sound amplitude variations in the audio sig-
285 nal spectrum, which can be observed in the form of characteristic patterns
286 of peak amplitudes. The underlying rationale in computing the FAV signa-
287 ture is to identify the peak patterns due to boats and ignore those related
288 to other acoustic events captured in the recordings. Our method identifies a
289 characteristic signature of each one-minute audio sample. It is thus possible
290 to distinguish the patterns due to boats from those originated from overlap-
291 ping acoustic events. Once the frequency peaks have been identified in the
292 FAV signature, a thresholding operation can be applied to obtain a binary
293 array with the boat detection signature.

294 Since our algorithm measures the differences in amplitude between neigh-
295 boring frequencies, it performs better with a standard spectrum in *dB* scale,
296 in which the amplitude variations are smoother. Measuring this frequency
297 variation along the audio spectrum will result in a characteristic signature
298 with amplitude peaks due to noticeable acoustic events. Operating on the
299 *dB* scale audio spectrum (Figure 2-A) facilitates distinguishing the peaks due
300 to boats from those introduced by other acoustic events.

301 Figure 3 illustrates two signatures computed with this approach for two
302 one-minute samples from the recordings depicted in the spectrograms in Fig-
303 ure 1. The charts show the spectrum signature (blue line), the FAV signature

304 (green line) and the boat detection signature (red vertical watermarks).

305 The signatures in Figure 3-A refer to the first minute of the recording
306 depicted in Figure 1-A, which includes a fish chorus overlapped with a ship
307 or large boat, whereas those in Figure 3-B refer to minute 11 in the recording
308 depicted in Figure 1-B, which includes a small boat and heavy noise due to
309 crustacean acoustic emission. One observes in the FAV signature in Figure 3-
310 A that only frequency peaks due to boats stand out, whereas other acoustic
311 events are largely ignored. The FAV and boat detection signatures depicted
312 in Figure 3-B show that the algorithm detected the faint signal of the small
313 boat even in the presence of heavy background noise.

314 Our method to process an input audio database consists of the following
315 steps. Given a root directory path containing the audio files to be processed,
316 first the signatures are computed for each individual recording applying Al-
317 gorithm 1, i.e., the spectrum, the frequency amplitude variation (FAV) and
318 the boat detection signatures. The resulting signatures for each file are stored
319 in a corresponding CSV file that preserves the source file name. The al-
320 gorithm also saves summary information on each boat detection signature,
321 namely the number of peaks identified, the shortest distance between the
322 peaks, and the lowest and highest amplitude peak values – this information
323 may be useful in further vessel classification procedures. The CSV signature
324 files are saved in a child folder of the root directory; the summary information
325 is stored in a single CSV file saved in the root directory.

326 The process requires two parameters: the sampling rate of the audio
327 recordings, which is known *a priori*, and a boat detection threshold. The
328 default threshold, which yielded good results in the databases studied, has

329 been set empirically to 1.5 times the standard deviation of the amplitude
330 spectrum of the signal. Thus, any peak that surpasses this threshold is
331 interpreted as a boat detection.

332 **Results**

333 The method has been validated on audio recordings collected at two sites
334 located on the West coast of the State of São Paulo, namely the Laje de
335 Santos Marine State Park (LSMSP, located at $24^{\circ}15'48"S$, $46^{\circ}12'00"W$) and
336 the Xixová-Japuí State Park (XJSP, located at $24^{\circ}0'22"S$, $46^{\circ}23'29"W$). Both
337 sites exhibit boat traffic and are characterized by great marine biodiversity.
338 The LSMSP is 30km (19 miles) off the coast and serves as a protected area
339 for reposition of fish shoals and safe reproduction of species. The XJSP
340 conservation unit encompasses a marine area SW of the Santos Bay and an
341 adjacent inland region of tropical forest. This is an area with strong human
342 presence, close to a very busy port in Brazil (Sánchez-Gendriz and Padovese,
343 2017; Sánchez-gendriz and Padovese, 2015).

344 The datasets consist of 15-minute monaural audio files recorded at a
345 sampling rate of 24 kHz. Recordings were obtained underwater with a custom
346 autonomous hydrophone recorder developed at LACMAN (Laboratory of
347 Acoustics and Environment of the Polytechnic School of the University of
348 São Paulo)¹.

349 In total, we analyzed 2,675 recordings from LSMSP and 2,390 recordings
350 from XJSP. As general observations, we noticed that the sound levels of the

¹<http://lacmam.poli.usp.br>

351 recordings taken at XJSP are, in average, $10dB$ higher than those taken at
352 LSMSP. This is possibly because XJSP is closer to the coast and has intense
353 boat traffic, whereas LSMSP is located in a quieter area farther away from
354 the coast. We also observed in some XJSP audio files a recording failure in
355 the low frequencies up to 100Hz. Both databases include many recordings
356 with multiple occurrences of diverse boats and ships, under different condi-
357 tions. Our goal was to assess the effectiveness of the proposed algorithm in
358 automatically detecting the presence of ships and boats on recordings collec-
359 ted from February 1 to February 28, 2015 (LSMSP site) and from February
360 4 to February 28, 2015 (XJSP site).

361 The spectrograms in Figures 4 and 5 depict, respectively, recordings taken
362 at two arbitrary days, namely February 17 at LSMP and February 10 at
363 XJSP. These particular days have been selected as illustrative examples of the
364 multiple acoustic events that can be found in both databases. The figures also
365 illustrate the outcome of the proposed boat detection algorithm. Detections
366 are displayed in the form of a line graph at the bottom and temporally aligned
367 with the corresponding audio spectrogram.

368 The red line indicates the boat detections at their exact location in time
369 along the duration of the audios, and also informs the number of frequency
370 amplitude peaks associated with the boat event, as detected by the algorithm.
371 In the examples, the number of peaks varied from 0 (no boat detected) up
372 to 5 peaks in the recordings taken at the LSMSP site (Figure 4); or from 0
373 up to 13 peaks in the recordings taken at the XJSP site (Figure 5).

374 The boat detections identified have been confirmed by listening to the
375 corresponding audio files. In all cases, a manual inspection confirmed the

376 automatic detection has been successful. In a few and very specific cases
377 false negatives occurred, with the algorithm failing to detect a boat that can
378 be identified in the audio; specific cases are discussed later in this section.

379 The boat detection line for the recordings from LSMS (Figure 4) shows
380 that the signatures of the boats detected in the early morning are charac-
381 terized by having one to three peaks and are not contiguous, whereas the
382 signatures of boats detected from 9:00am onwards are characterized by more
383 peaks which are also very close – these usually correspond to a series of short
384 duration acoustic events.

385 Observing the recordings from XJSP (Figure 5), one notices that longer
386 duration acoustic events associated with boats are frequent during certain
387 morning and evening periods. The boat detection line chart reveals multiple
388 short duration boat events occurring frequently from nearly 9:00am until
389 dusk. Short-term boat events have also been detected in the early morning,
390 before 9:00am, and during the evening, after 6:00pm. After 6:30pm, when
391 an overlapping fish chorus event is visible in the spectrogram, multiple boat
392 events have been detected with signatures characterized by higher numbers
393 of peaks. From 10:00pm it is possible to observe a long duration boat event
394 that persists until midnight.

395 Acoustic events typical of the site, such as fish choruses, can mask some of
396 the peaks characteristic of a boat signature, as frequency peaks of both events
397 overlap. They can still be distinguished by further inspecting the differences
398 in the amplitudes of the neighboring frequencies. Nonetheless, the overlap
399 may cause boat peaks at these frequencies to go undetected. In these cases,
400 successful detection depends on a proper choice of the detection threshold

401 defined relative to the standard deviation of the spectrum signature, which
402 is the single setting of the automatic detection process that may require user
403 adjustment.

404 Figure 6 shows an example in which a long duration boat event has been
405 detected. The boat detection line chart appears as a line with a constant
406 number of peaks over a range of frequencies, which persists during nearly
407 the entire duration of the recording. The detection line chart shows two to
408 three peaks along minutes 1 to 9. The peaks overlap with the frequencies of
409 a simultaneous fish chorus event.

410 The audio of the spectrogram in Figure 7 includes an acoustic event oc-
411 curring from minutes 7 to 12, approximately. Listening to the audio one
412 observes the sound of (apparently) a motor boat that gradually approaches
413 the hydrophone and then its engine is turned off. The boat signature detec-
414 ted has a varying number of peaks: an initial detection indicates 3 peaks,
415 followed by a short period with no detection; the boat is again detected with
416 a signature of 8 peaks, going up to 12 peaks in minute 11, then in minute 12
417 only a single peak is detected, when the engine is powered off. The varying
418 number of peaks is due to the non uniform properties of the sound emission by
419 the boat. Its signal amplitude increases as it approaches the hydrophone and
420 fades away when the engine is suddenly turned off. The algorithm success-
421 fully detected the boat, despite the unfavourable conditions and overlapping
422 acoustic noise from a fish chorus.

423 Another difficult case for the algorithm is illustrated in Figure 8, in which
424 the audio depicts a short duration and non-uniform sound emission by a boat,
425 which is masked by extensive background noise due to crustacean acoustic

426 activity. Nonetheless, the algorithm managed to achieve a partial recognition,
427 as indicated by the detection line graph, in minutes 5 and 6. Only one of
428 the peaks of the boat signature has been identified, due to the short interval
429 between the acoustic events and the overlapping noise.

430 A particular case in which the algorithm failed to detect the boat sig-
431 nature is shown in Figure 9, which depicts an audio that includes a boat
432 with non-constant acceleration. In this case, the frequencies of the spectral
433 signature do not exceed the default threshold that indicates a positive boat
434 detection. The acoustic event occurred in minute 12 of the recording, going
435 undetected due to the insufficient duration of the peaks in a single frequency.

436 Many boat occurrences have been detected in the recordings taken at
437 the LSMP site, even though boat visitation is controlled or even prohibited
438 at certain periods. Interestingly, from February 10 to 28 long-term acoustic
439 emissions by boats are detected often in the mornings, mostly boat signatures
440 characterized by up to two peaks. These emissions are low amplitude signals
441 and the boats are apparently located distant from the hydrophone. Yet the
442 algorithm successfully detected such occurrences, even though the recorded
443 signal often includes multiple acoustic events in addition to the boats.

444 Other cases confirm the effectiveness of the proposed algorithm. Consider,
445 for example, the audio illustrated in the spectrogram in Figure 10. The
446 algorithm detected a boat signature characterized by a single frequency peak
447 in this recording. This was a particularly challenging case, because the boat
448 signal was faint and heavily masked by a loud noise due to crustacean acoustic
449 activity.

450 A second example is illustrated in Figure 11, which depicts an audio in

451 which the algorithm detected a boat signature characterized by 35 to 59
452 peaks along the duration of the recording. Although we cannot estimate the
453 distance of the boat to the hydrophone, its signal is sufficiently loud for its
454 signature to be properly detected even above the 1KHz frequency band.

455 Yet another challenging example are cases of multiple boats captured
456 in the same recording, possibly as overlapping acoustic events. The audio
457 spectrogram in Figure 12 shows a boat event that persists along the duration
458 of the recording, however a second boat event occurs in minutes 4 to 6.
459 This is difficult to handle due to the overlap of both boat signatures. The
460 signatures computed for the audio samples depicting minutes 2 to 5 are
461 shown in Figure 12 to illustrate how multiple events interfere in the detection
462 process. In the signatures of minutes 2 and 3 one observes the complete and
463 the partial signatures of the persistent boat; in minute 4 the transient boat
464 event partly masks the previous signature, introducing additional peaks. The
465 emission by the transient boat in minute 5 is sufficient to mask the signature
466 of the persistent boat, as it adds noise in the frequency band from 200Hz to
467 2kHz. The consequence is that only the signature of the transient boat is
468 detected.

469 Comparison: FAV vs DEMON

470 A DEMON implementation based on square-law demodulation by Pollara
471 et al. (2016) available online² has been used as baseline for a comparison with
472 the proposed FAV signature, regarding detection accuracy and processing

²<https://github.com/lxpollara/pyDEMON>

473 times. The code and audio samples used in the analysis and comparisons
474 can be downloaded from github (Reis, 2019).

475 We conducted the comparison on 96 audio files selected from our data-
476 bases (Xixová and Japuí State Parks), corresponding to 24 hours of au-
477 dio analysed at a one-minute sample resolution, totaling 1,440 one-minute
478 samples representative of typical scenarios found in underwater ecological
479 recordings. We conducted a manual annotation process and identified that
480 from the 1,440 samples considered, 706 do not include boat events, whereas
481 the remaining 734 include diverse observable boat occurrences, varying from
482 very clear to very faint signals. The samples depict distinct situations, in-
483 cluding non-uniform vessel emissions near the hydrophone and other difficult
484 scenarios characterized by overlapping with crustacean acoustic emissions or
485 fish choruses.

486 The DEMON signature computation requires the definition of a target
487 frequency window for each detection scenario. Inadequate choice of this
488 initial input parameter can render the detection task unfeasible. In order to
489 ensure a proper comparison, the input samples were processed similarly for
490 both methods, setting the higher frequency to 900Hz and the low frequency
491 to 400Hz as the default parameters for the DEMON signature calculations.
492 Each one-minute sample was smoothed with a size 11 Blackman window
493 convolution, and the corresponding standard deviations were extracted.

494 In both methods, a detection occurs whenever the corresponding signa-
495 ture exceeds the corresponding detection threshold, where each excess will
496 correspond to a frequency peak in the boat detection signature. We kept the
497 default detection threshold for the FAV signature, i.e., $1.5 \times \text{standard deviation}$.

498 Setting the detection threshold for DEMON requires a different approach,
499 however, as the base signals vary in amplitude due to interference of noise.
500 Thus, we set an initial threshold as in FAV ($1.5 \times \text{standard deviation}$), then
501 obtained a basis amplitude for each frequency by smoothing the DEMON sig-
502 nature with a size 64 Blackman window convolution. The basis amplitudes
503 thus obtained were then added to the initial threshold.

504 Under normal conditions these threshold settings enabled both methods
505 to correctly detect the presence of boats and create the corresponding boat
506 signatures. An example for a particular one minute sample is illustrated in
507 Figure 13, where a boat with two frequency peaks can be observed, which
508 has been correctly detected in both FAV and DEMON signatures. However,
509 results from the methods differ in more challenging conditions. Detection
510 results for a noisy sample are illustrated in Figure 14, where FAV correctly
511 identified a boat with eight frequency peaks. The DEMON signature, how-
512 ever, detected only one of the peaks and also incurred in a false positive
513 detection of a frequency peak which is not due to a boat.

514 Considering all 1,440 samples, we computed the detection accuracy and
515 the correctness of the number of peaks identified in the signatures obtained
516 from both methods. Detection accuracy is reported as the numbers and
517 percentages of correct and incorrect boat detections. The signature accuracy
518 is measured as the number of detected frequency peaks, relative to the true
519 number of peaks. We report the average percentages for each method, over
520 all signatures extracted.

521 Table 1 shows two confusion matrices displaying the detection accuracy
522 results for the FAV and the DEMON implementations, respectively. The

523 columns labeled **Reality** inform the number of boat occurrences according
524 to the manual annotation, the rows labeled **Algorithm** show the results
525 obtained with FAV or DEMON. Table 2 summarizes the accuracy rates and
526 also the false positive and false negative rates.

527 FAV correctly detected the presence of boats in 684 out of the 734 samples
528 with boat occurrences, an accuracy rate of 93%. It missed 50 occurrences,
529 and incurred in no false positives. DEMON correctly detected 406 boat occur-
530 rences, an accuracy rate of 55%. It missed 328 boat events, and incorrectly
531 detected 84 acoustic events as boats. The **false-negative** rates in our ana-
532 lysis of DEMON could be disputed, since the manual annotation identified
533 some very faint boat signals. Possibly different calibrations of DEMON would
534 be required for it to perform better on the database as a whole, as the condi-
535 tions describing boat events vary considerably. On the other, FAV has shown
536 very robust performance with the settings employed, regardless of the varied
537 conditions.

538 For the 734 samples including boat occurrences we also computed the
539 correctness of the number of frequency peaks identified, as a measure of the
540 quality of the signatures computed. For instance, given a boat signature
541 with 5 frequency peaks, if a method computes the signature with 3 peaks, its
542 resulting signature accuracy is 60%. As informed in Table 2 (second row),
543 the average signature accuracy of the FAV method over all samples was 80%,
544 whereas for the DEMON method it was 29%.

545 Table 3 shows the times, in seconds, to extract the DEMON and FAV
546 signatures for a 15 minute audio recording and for a one minute sample of the
547 same recording, considering five executions of the algorithm implementations.

548 In the 15 minute sampling we observe a speed up of nearly 230, as the average
549 execution times drop from 6.743 seconds to compute the DEMON signature
550 to 0.029 seconds to compute the FAV signature. In the one minute sample
551 the DEMON signature has been computed in 0.416 seconds in average, and
552 the FAV signature in 0.006 seconds, a speed up of nearly 70.

553 These empirical investigations provide evidence on the improved perform-
554 ance of the FAV algorithm over the DEMON implementation, regarding both
555 computational cost and accuracy, the later measured in terms of detection
556 correctness and signature quality. Moreover, unlike DEMON, FAV requires
557 no specific settings or prior knowledge of the boat frequency signatures. It
558 is a self-contained solution that relies solely on the input signal of the au-
559 dio spectrum. A single user setting is required to establish the detection
560 threshold, where the default setting as $1.5 \times \text{Standard Deviation}$ of the
561 original spectrum proved adequate in all cases appearing in the databases
562 considered.

563 **Summary**

564 In this paper we introduced FAV, a method to detect the presence of ves-
565 sels in underwater ecological acoustic recordings. Results from experiments
566 conducted on recordings collected in February 2015 at two sites in Brazil
567 provide empirical evidence on its effectiveness. The examples discussed show
568 the method can successfully detect the presence of boats even in difficult
569 conditions, such as faint signals and multiple overlapping acoustic events.
570 Manual inspection of all the recordings considered in the experiments re-

571 vealed no false positives and a small rate of missed detections in very specific
572 situations.

573 The algorithm can recognize boats under constant acceleration, where the
574 resulting sound signal caused by cavitation generates characteristic peaks
575 at short frequency intervals. The failure cases were of boats with erratic
576 acceleration behavior. This situation shall be addressed in further work,
577 possibly with an analysis of the amplitude variation in time, combined with
578 frequency information and machine learning methods to recognize specific
579 patterns.

580 Besides detecting emissions by boats and ships, the FAV signature is also
581 susceptible to sound emission by airgun arrays. The reason is that such
582 devices produce acoustic energy with frequency amplitudes mostly under
583 100Hz (Hermannsen et al., 2015; Landro et al., 2011), the same band of the
584 boat emissions. For boat detection purposes, if an acoustic signal emitted
585 by an airgun array is identified one can assume the consequent detection of
586 a boat signal, since airgun arrays are towed by boats.

587 In comparison with the classic DEMON method, which also relies on
588 analysis of the acoustic signal for boat detection, our solution provides an al-
589 ternative that is easy to implement and does not require extensive processing
590 power or complex configuration of input parameters. DEMON, on the other
591 hand, requires human intervention to define the best filters for each type of
592 target signal and is computationally more expensive.

593 In future work we intend to tackle the problem of boat classification
594 based on their characteristic FAV signatures. We believe classification would
595 be feasible with a combination of machine learning and data visualization

596 methods integrated into a visual analytics solution that supports user steer-
597 ing. The simultaneous detection of multiple ship signatures is another chal-
598 lenging task that deserves further attention.

599 **Authors' contributions**

600 Clausius Reis conceived the ideas, designed the methodology and imple-
601 mented the proposed algorithms; Linilson Padovese collected the underwa-
602 ter data; Clausius Reis and Maria Cristina analysed the data and results;
603 Clausius Reis and Maria Cristina led the writing of the manuscript. All au-
604 thors discussed the results, contributed critically to the drafts and gave final
605 approval for publication.

606 **Acknowledgements**

607 The authors acknowledge the financial support of the São Paulo State Re-
608 search Foundation (FAPESP grants 2017/05838-3 and 2016/02175-0) and
609 the National Council for Scientific and Technological Development (CNPq
610 grant 301847/2017-7). The views expressed do not reflect the official policy
611 or position of either FAPESP or CNPq.

612 **Data Accessibility**

613 The data and codes used on this paper are available under GPL-3.0 license
614 at <https://doi.org/10.5281/zenodo.3252202> (Reis, 2019).

615 References

616 Averbuch A, Zheludev V, Neittaanmäki P, Wartiainen P, Huoman K, Janson K.
617 2011. Acoustic detection and classification of river boats. *Applied Acoustics* **72**:
618 22 – 34. ISSN 0003-682X.

619 Chung KW, Sutin A, Sedunov A, Bruno M. 2011. DEMON acoustic ship signature
620 measurements in an urban harbor. *Advances in Acoustics and Vibration* **2011**.
621 URL <http://doi.org/10.1155/2011/952798>

622 Hanson D, Antoni J, Brown G, Emslie R. 2008. Cyclostationarity for Passive Un-
623 derwater Detection of Propeller Craft: A Development of DEMON Processing.
624 *Proceedings of Acoustics November*: 1–6.

625 Hermannsen L, Tougaard J, Beedholm K, Nabe-nielsen J. 2015. Characteristics and
626 Propagation of Airgun Pulses in Shallow Water with Implications for Effects on
627 Small Marine Mammals. *PLOS ONE July*: 1–17.
628 URL <https://doi.org/10.1371/journal.pone.0133436>

629 Jain-Schlaepfer S, Fakan E, Rummer JL, Simpson SD, McCormick MI, Cooke S.
630 2018. Impact of motorboats on fish embryos depends on engine type. *Conserv
631 Physiol* **6**: 1410–1093.
632 URL <https://doi.org/10.1093/conphys/coy014>

633 Landro M, Amundsen L, Barker D. 2011. High-frequency signals from air-gun
634 arrays. *Geophysics* **76 NO. 4**: Q19–Q27.
635 URL <http://dx.doi.org/10.1190/1.3590215>

636 Leal N, Leal E, Sanchez G. 2015. Marine vessel recognition by acoustic signature.
637 *ARPN Journal of Engineering and Applied Sciences* **10**: 9633–9639.

638 Merchant ND, Pirotta E, Barton TR, Thompson PM. 2014. Monitoring ship noise
639 to assess the impact of coastal developments on marine mammals. *Marine Pol-
640 lution Bulletin* **78**: 85–95.
641 URL <https://doi.org/10.1016/j.marpolbul.2013.10.058>

642 Pollara AS, Lignan G, Boulange L, Sutin A, Salloum H. 2017. Specifics of demon
643 acoustic signatures for large and small boats. *The Journal of the Acoustical
644 Society of America* **141**: 3991–3991.
645 URL <https://doi.org/10.1121/1.4989137>

646 Pollara AS, Sutin A, Salloum H. 2016. Improvement of the Detection of Envelope
647 Modulation on Noise (DEMON) and its application to small boats. *OCEANS
648 2016 MTS/IEEE Monterey, OCE 2016* : 1–10.
649 URL <http://doi.org/10.1109/OCEANS.2016.7761197>

650 Reis CDG. 2019. FAV-Signature. <https://github.com/clausiusreis/FAV-Signature>. [Online; accessed 24-March-2019].

651 URL <https://doi.org/10.5281/zenodo.3252202>

653 Sánchez-gendriz I, Padovese LR. 2015. Underwater soundscape of marine protected areas in the coastal of Sao Paulo, Brazil. *Marine Pollution Bulletin* **105**: 65–72.

654 URL <http://doi.org/10.1016/j.marpolbul.2016.02.055>

655 Sánchez-Gendriz I, Padovese LR. 2017. Temporal and spectral patterns of fish choruses in two protected areas in southern Atlantic. *Ecological Informatics* **38**: 31–38.

656 URL <https://doi.org/10.1016/j.ecoinf.2017.01.003>

657 Slamnoiu G, Radu O, Rosca V, Pascu C, Damian R, Surdu G, Curca E, Radulescu A. 2016. DEMON-type algorithms for determination of hydro-acoustic signatures of surface ships and of divers. *IOP Conference Series: Materials Science and Engineering* **145**.

658 URL <https://doi.org/10.1088/1757-899X/145/8/082013>

659 Tuteur FB. 1963. *Detection of wide-band signals modulated by a low-frequency sinusoid*. Appendix A-4, New Haven, Conn, USA: Yale University.

660 Veirs S, Veirs V, Wood JD. 2016. Ship noise extends to frequencies used for echo-location by endangered killer whales. *PeerJ* **4**: e1657.

661 URL <https://doi.org/10.7717/peerj.1657>

662 Wittekind D, Schuster M. 2016. Propeller cavitation noise and background noise in the sea. *Ocean Engineering* **120**: 116–121.

663 URL <http://dx.doi.org/10.1016/j.oceaneng.2015.12.060>

664 Yan J, Sun H, Cheng E, Kuai X, Zhang X. 2017. Ship radiated noise recognition using resonance-based sparse signal decomposition. *Shock and Vibration* **2017**.

675 **Tables**

Table 1 Detection accuracy of FAV and DEMON algorithms on a database of 1,440 one minute audio samples.

Confusion matrix FAV				Confusion matrix DEMON			
Algorithm	Reality		# Samples	Reality		# Samples	
	NO Boat	Boat		No Boat	Boat		
NO Boat	706	50	706	622	328	706	
Boat	0	684	734	84	406	734	
# Samples	706	734					

Table 2 Boat detection accuracy and signature accuracy results obtained with the FAV and DEMON implementations, as well as false positive and false negative detection rates.

	FAV	DEMON
Detection accuracy	93.19%	55.31%
Signature accuracy	80.38%	29.21%
% of false positives	0.00%	10.63%
% of false negatives	20.42%	45.14%

Table 3 Times (in seconds) to compute the boat signatures of a 15 minute audio recording and of a one minute sample extracted from the same audio. Time measures were obtained from five executions of each (DEMON/FAV) implementation on a *Intel*® *Core*™ *i7* – 7700 @ 3.60GHz × 4 with 16GB memory.

Time (Seconds)	15 minute audio		One minute audio	
	DEMON	FAV	DEMON	FAV
6.672	0.031	0.413	0.006	
6.760	0.029	0.421	0.006	
6.743	0.030	0.416	0.006	
6.790	0.027	0.431	0.006	
6.606	0.029	0.409	0.006	
Avg	6.743	0.029	0.416	0.006

676 **Figures**

Fig. 1 Logarithmic scale spectrograms of two underwater recordings. The red squares mark frequency peaks due to boats and the blue squares mark peaks due to fish choruses. Both recordings include background noise due to acoustic emission by crustaceans, that can be perceived as vertical lines in the spectrograms. (A) 15-minute audio spectrogram with two types of fish chorus and a boat signature characterized by three peaks; (B) 15-minute spectrogram with a single boat signature characterized by 10 peaks and heavy background noise due to crustacean emissions.

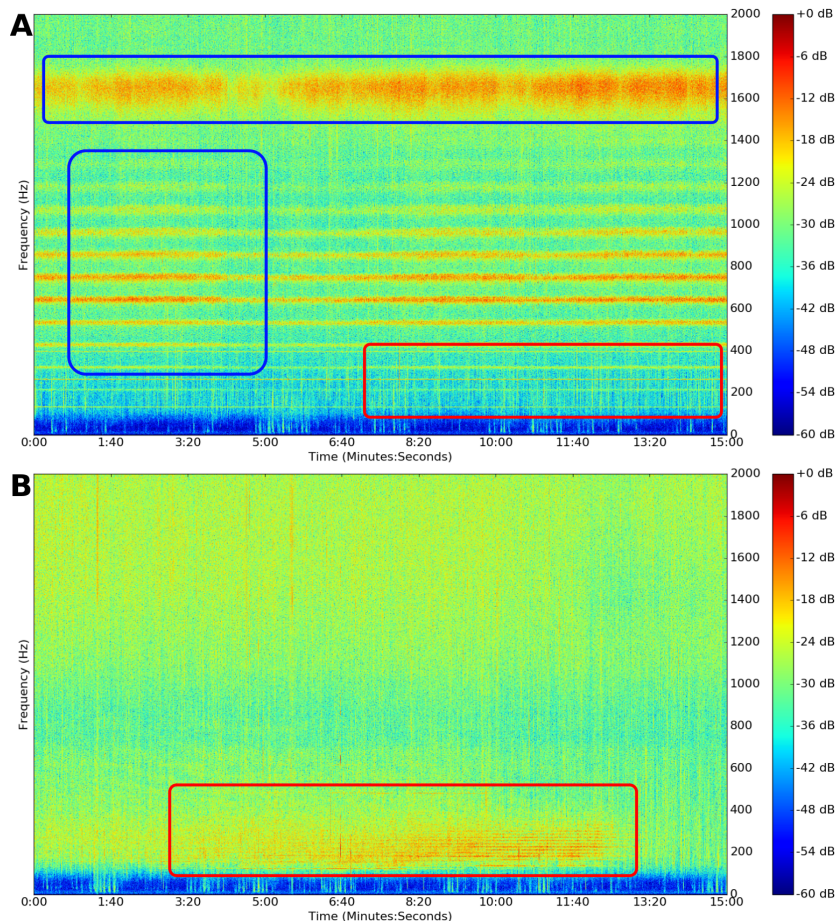


Fig. 2 In both charts the blue lines depict, respectively, the frequency spectra (up to 2.7kHz) of an input signal in dB (A) and in dB^2 (B); the green and red dotted lines depict the spectral signal smoothed by convolution with a size 11 blackman window, scaled respectively by $1.5 \times$ and by $3 \times$ its standard deviation. The vertical watermarks in red identify the frequency peaks due to boat emissions.

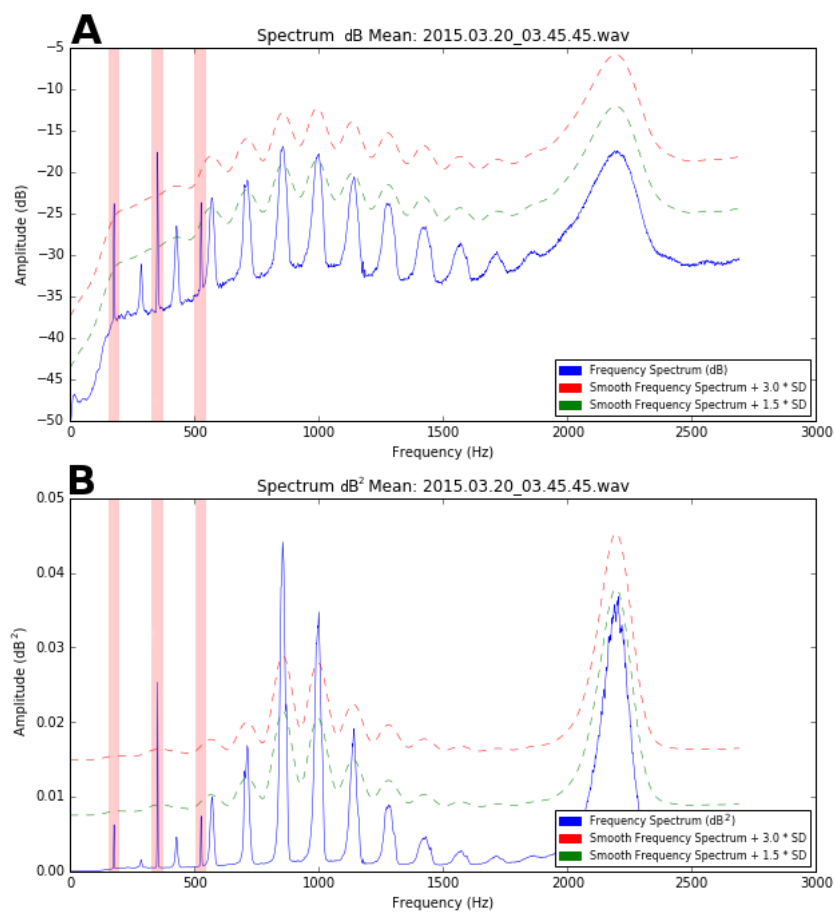


Fig. 3 Spectrum signature (blue line), FAV signature (green line) and binary boat detection signature (red marks) of (A) a recording that includes fish chorus and a boat; and (B) a recording that includes a small boat at minute 11. The horizontal dotted purple lines indicate the threshold defined to associate frequency peaks with acoustic emissions by boats.

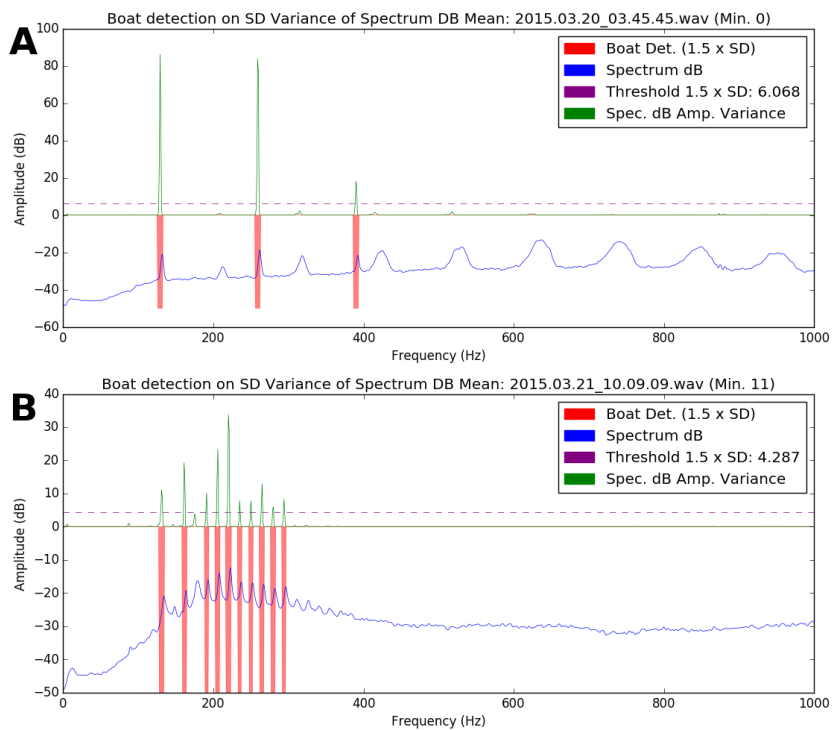


Fig. 4 24-hour spectrogram (frequency band from 0 to 2KHz) of the audio recordings taken at LSMSp in February 17, 2015. The recordings captured three types of fish chorus (A, B and C), as well as long and short duration sound emissions by boats and ships (D). The line chart at the bottom shows the detections obtained with the proposed method minute-by-minute and the number of peaks that characterize the corresponding boat signature.

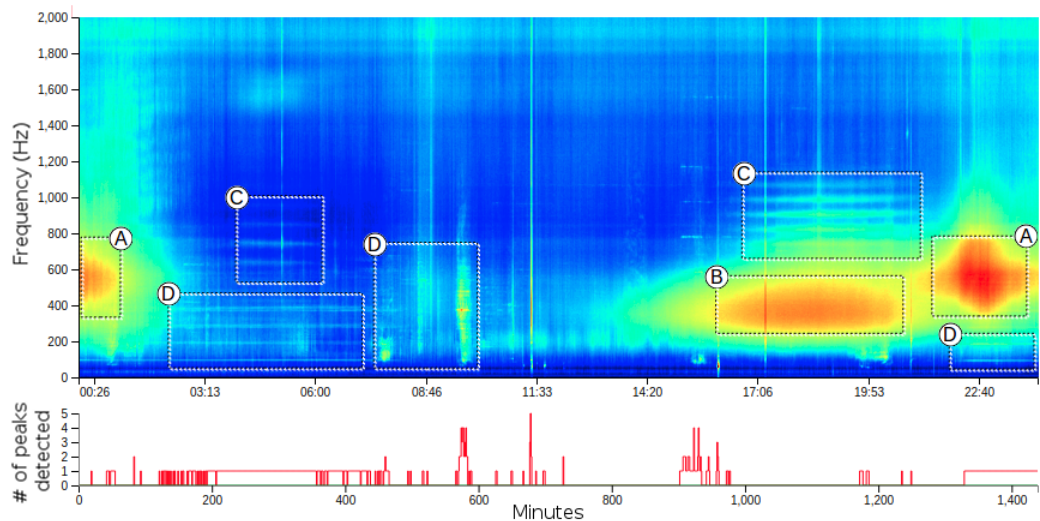


Fig. 5 24-hour spectrogram (frequency band from 0 to 2KHz) of audio recordings taken at XJSP in February 10, 2015. The recordings captured three types of fish choruses (A, B and C) and sound emissions by multiple ships (D) appearing as long and short duration acoustic events. The detection line chart shown under the spectrogram reveals a concentration of short duration boat events in the period from around 9:00am to 11:00am; their corresponding signatures are characterized by up to 13 frequency peaks.

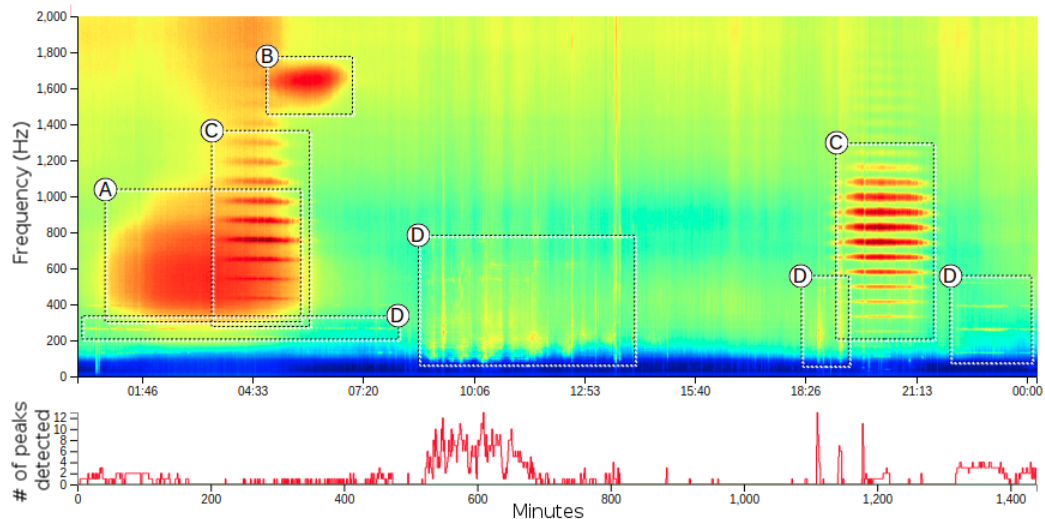


Fig. 6 15-minute spectrogram (frequency band from 0 to 1KHz) of a recording taken at XJSP in February 4, 2015 at 05h:39m:52s. A boat has been detected in the interval from minutes 1 to 9; the corresponding boat detection line chart is shown at the bottom.

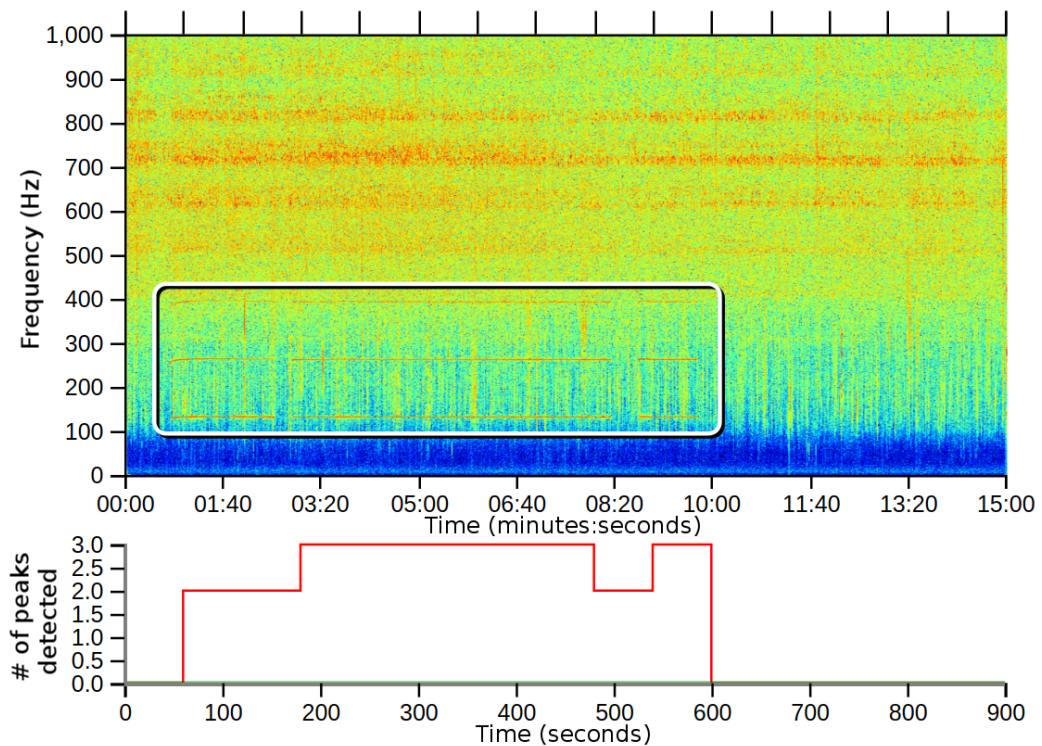


Fig. 7 15-minute spectrogram of a recording taken at XJSP in February 4, 2015 at 21h:12m:44s (frequency band from 0 to 1KHz). A boat occurrence has been detected in the interval from minutes 7 to 12; the corresponding boat detection line chart is shown at the bottom.

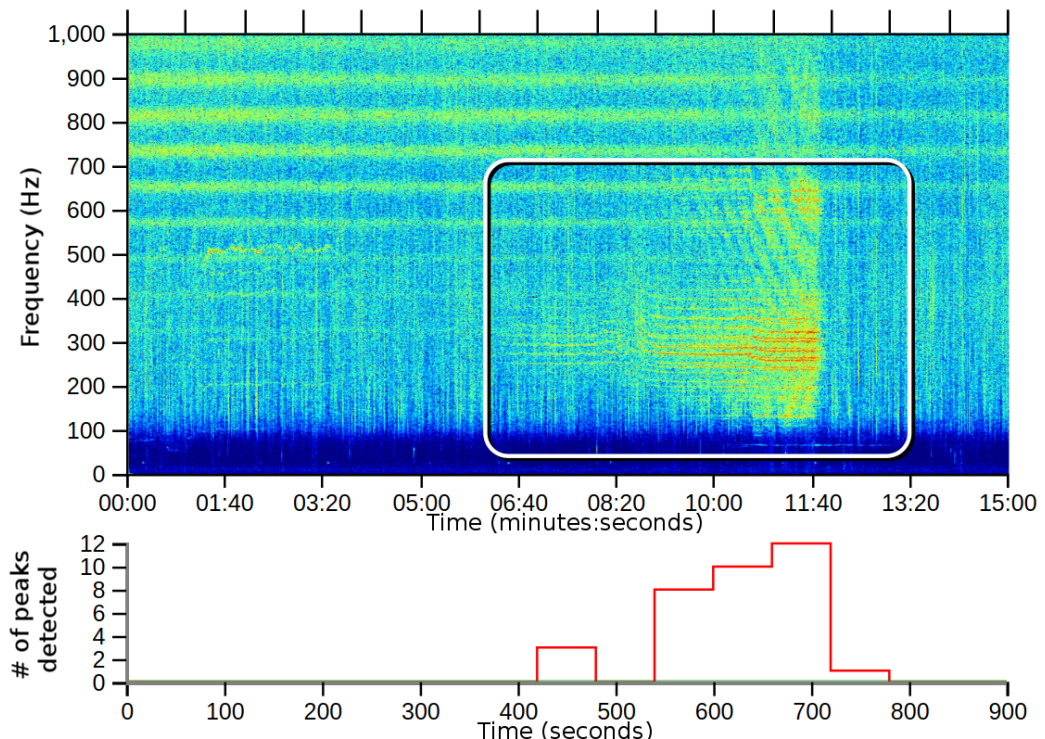


Fig. 8 15-minute spectrogram (frequency band from 0 to 1KHz) of a recording taken at XJSP in February 4, 2015 at 10h:40m:46s, in which a boat has been detected during minutes 5 and 6; the corresponding boat detection line chart is shown at the bottom.

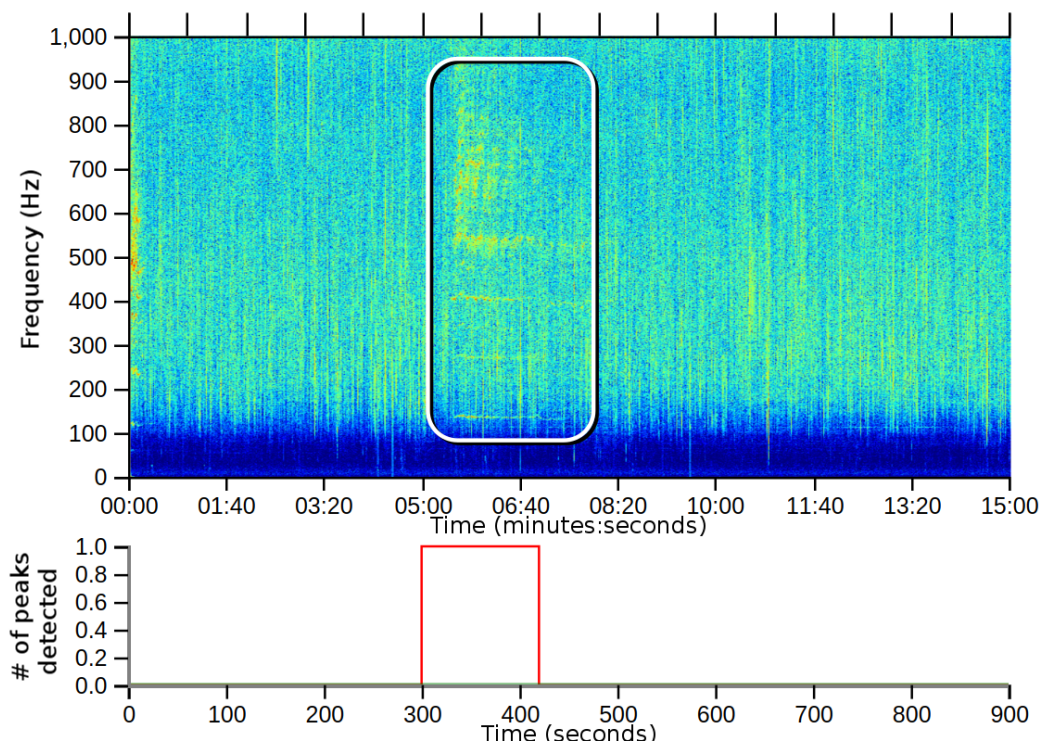


Fig. 9 15-minute spectrogram (frequency band from 0 to 1KHz) of a recording taken at XJSP in February 4, 2015 at 10h:10m:42s. Listening to the audio it is possible to identify the sound of a boat at minute 12, which the algorithm failed to detect, as observed in the corresponding detection line chart at the bottom.

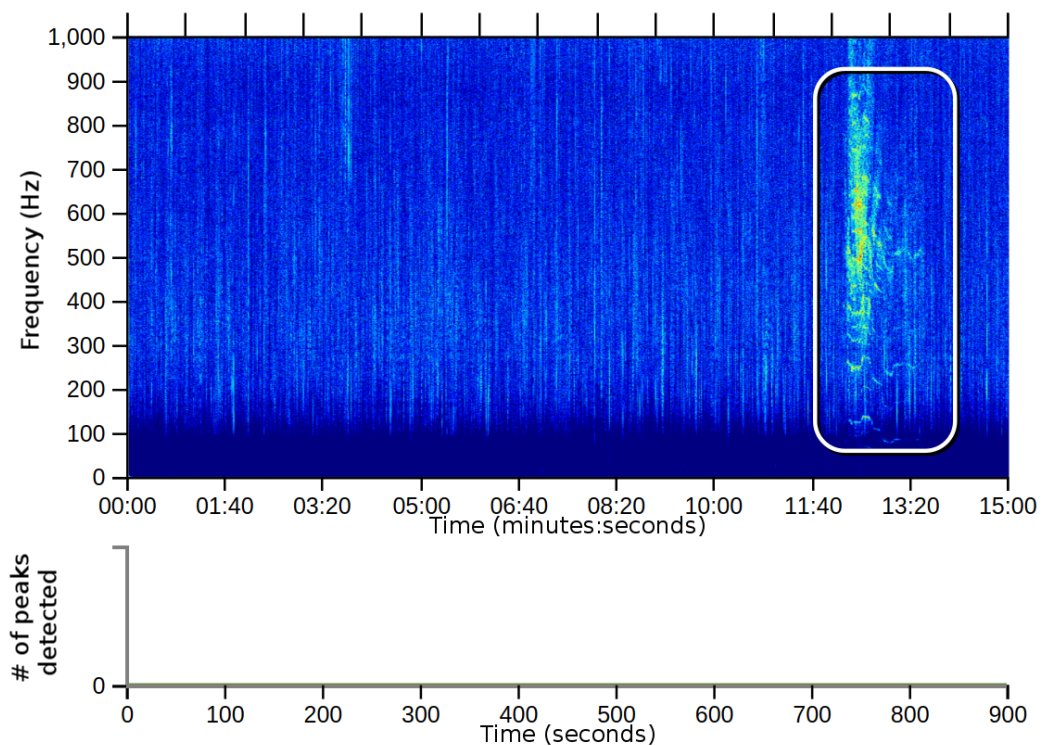


Fig. 10 15-minute spectrogram (frequency band from 0 to 1KHz) of a recording taken at LSMP in February 11, 2015 at 06h:27m:57s. The low amplitude signal from a boat has been detected in the intervals from minutes 0 to 3 and from 8 to 11, even though it is masked by crustacean noise, as observed in the boat detection line chart shown at the bottom.

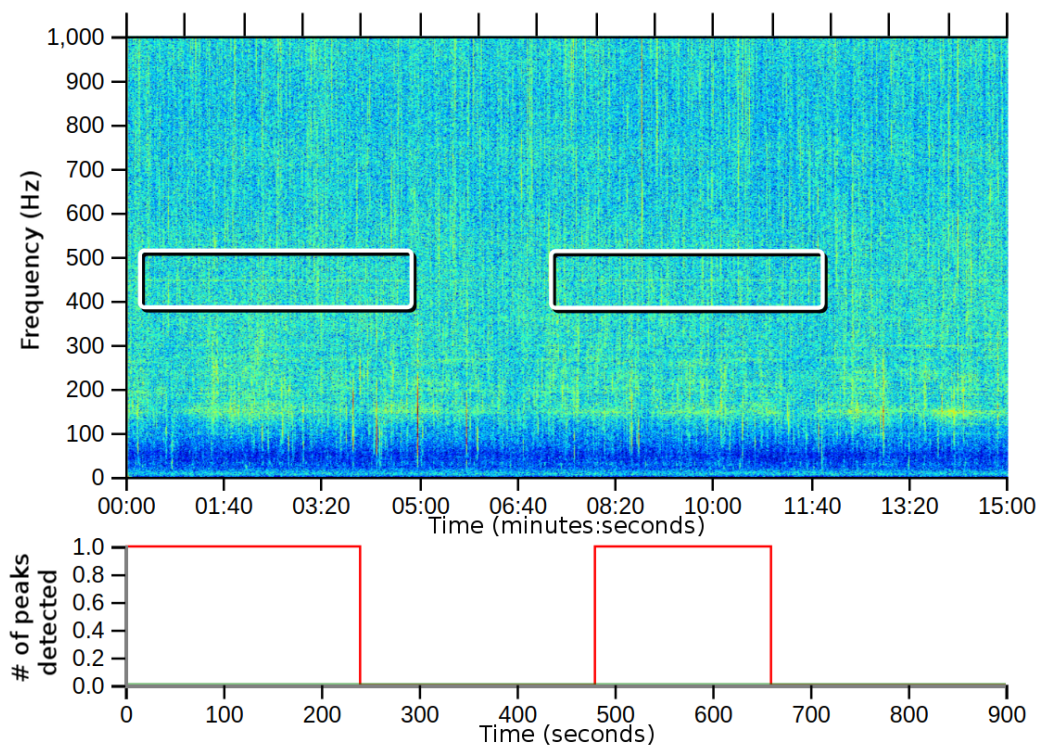


Fig. 11 15-minute spectrogram (frequency band from 0 to 1KHz) of a recording taken at LSMSp in February 11, 2015 at 15h:29m:54s. The signature of a boat has been detected along the duration of the recording, characterized by 35 up to 59 frequency peaks, as observed in the corresponding detection line chart.

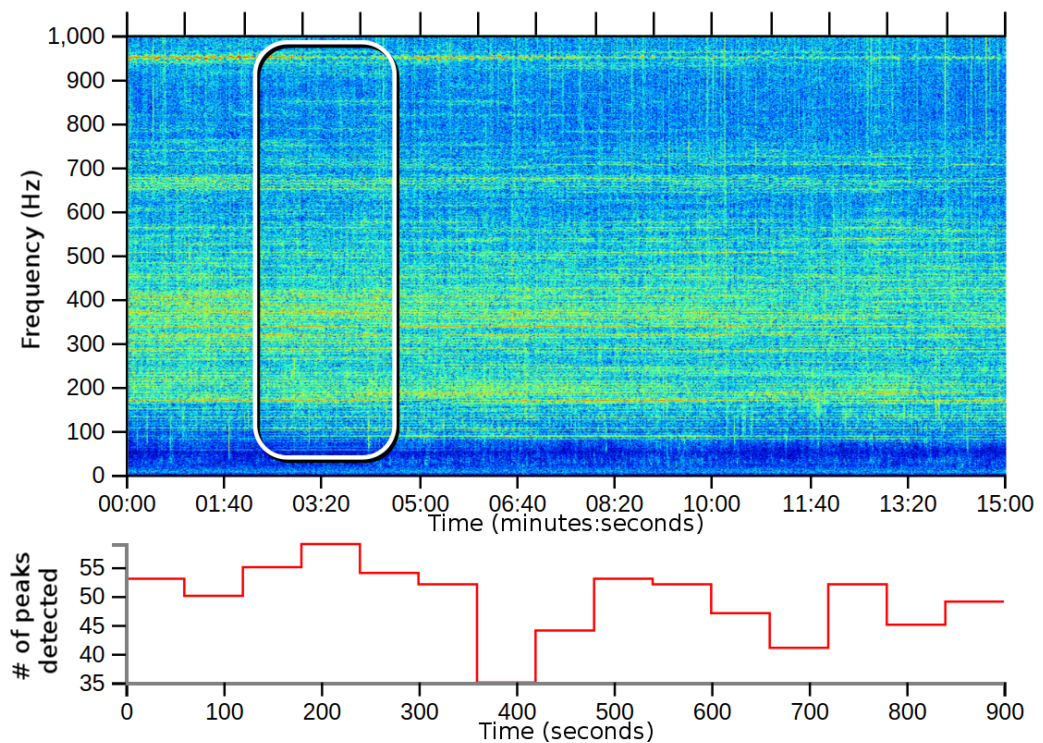


Fig. 12 15-minute spectrogram of a recording taken at LSMSP in February 4, 2015 at 04h:48m:55s, where overlapping sound emissions from two boats can be observed. The charts show the signatures computed of the audio samples corresponding to minutes 2, 3, 4 and 5, displaying the input spectrum signature (blue lines) with the corresponding boat detections highlighted by the red vertical lines.

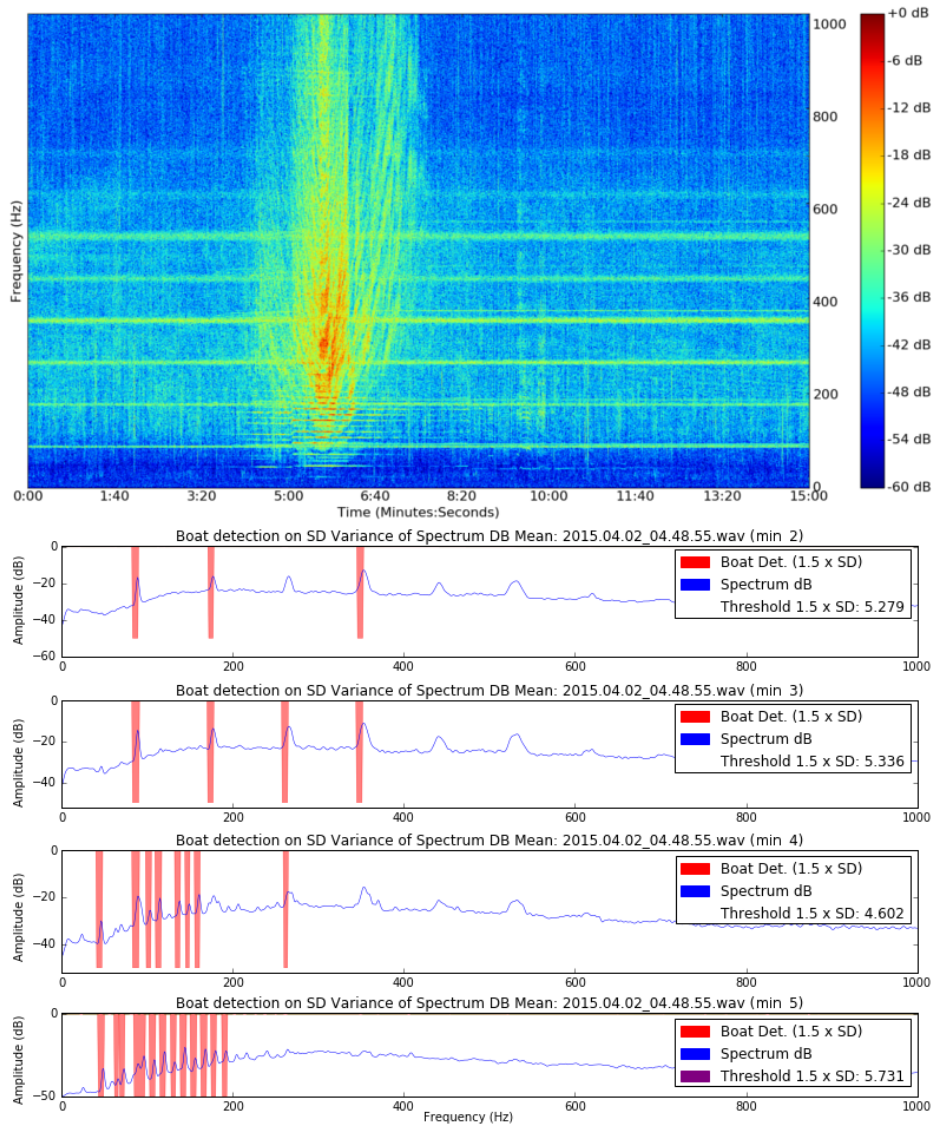


Fig. 13 FAV and DEMON signatures obtained for a one-minute audio sample that includes crustacean acoustic activity overlaped with a persistent acoustic emission by a boat (spectrogram on the right). The dotted gray lines indicate the detection threshold ($1.5 \times \text{Standard Deviation}$). Both algorithms correctly detected the boat signature, with two frequency peaks. The red watermarks indicate the peaks detected in the FAV signature (purple line); the black dots indicate the detections in the DEMON signature (green line).

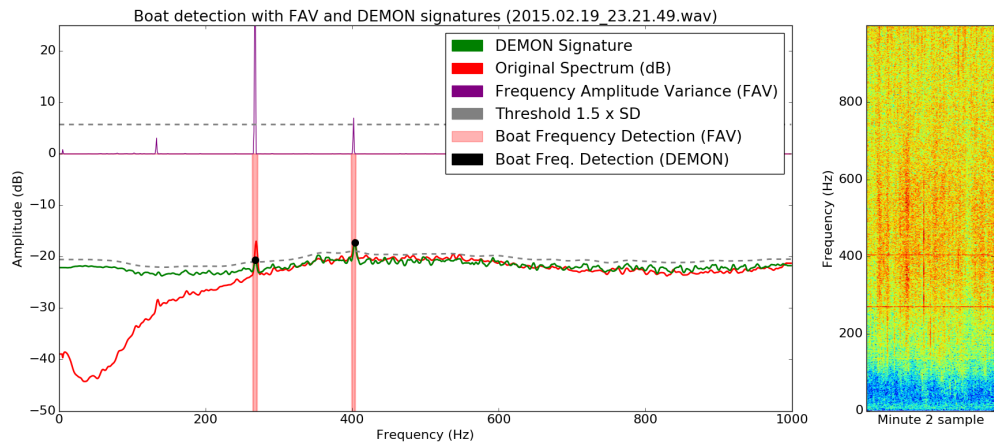


Fig. 14 FAV and DEMON signatures obtained for a one-minute audio sample that includes crustacean acoustic activity overlaped with a persistent acoustic emission by a boat (spectrogram shown on the right). The dotted gray lines indicate the detection threshold ($1.5 \times \text{Standard Deviation}$). In this case the boat signature is characterized by eight frequency peaks. The red watermarks indicate the boat peaks correctly detected in the FAV signature (purple line); the black dots indicate the detections in the DEMON signature (green line). The DEMON algorithm identified a single peak due to the boat, the other peak is actually a false-positive, not related to the boat.

